ISSN 1063-7788, Physics of Atomic Nuclei, 2009, Vol. 72, No. 2, pp. 214–230. © Pleiades Publishing, Ltd., 2009.
Original Russian Text © V.V. Varlamov, N.N. Peskov, M.E. Stepanov, 2009, published in Yadernaya Fizika, 2009, Vol. 72, No. 2, pp. 241–257.

NUCLEI
Experiment

Special Features of the Isospin Splitting of the Giant Dipole Resonance in the ^{90}Zr Nucleus

V. V. Varlamov*, N. N. Peskov, and M. E. Stepanov

Institute of Nuclear Physics, Moscow State University, Moscow, 119991 Russia

Received March 26, 2008; in final form, July 8, 2008

Abstract—Data on the proton and neutron channels of the ^{90}Zr photodisintegration were analyzed in detail, basic parameters of the isospin splitting of the giant dipole resonance in ^{90}Zr being determined by the properties of these channels. New data concerning the cross sections for the partial photoneutron reactions $^{90}\mathrm{Zr}(\gamma,n)^{89}\mathrm{Zr}$ and $^{90}\mathrm{Zr}(\gamma,2n)^{88}\mathrm{Zr}$ and resulting from a simultaneous correction of data from experiments performed in Livermore (USA) and Saclay (France) by using beams of quasimonoenergetic annihilation photons were invoked. Use was made of information about the positions on the energy scale of states characterized by different isospin values in the ^{90}Zr nucleus and nuclei neighboring it, which are members of the respective isospin multiplet. New data on the parameters of the isospin splitting of the giant dipole resonance in the ^{90}Zr nucleus were obtained on the basis of a global analysis of data on the giant-dipole-resonance states of the ^{90}Zr nucleus, which are manifested in the respective photoneutron and photoproton cross sections and in their decay channels involving states of different isospin in neighboring nuclei.

PACS numbers: 29.85.-c
DOI: 10.1134/S1063778809020033

1. INTRODUCTION

In [1], our group analyzed, for a large number of nuclei, experimental data on the isospin splitting of the giant dipole resonance (GDR),

$$\Delta E = E_{\mathrm{c}}(T_>) - E_{\mathrm{c}}(T_<), \qquad (1)$$

where $E_{\mathrm{c}}(T_>)$ and $E_{\mathrm{c}}(T_<)$ are the energy centroids of the components $\sigma^>$ and $\sigma^<$ of the cross sections for reactions that contribute to the respective GDR components of isospin $T_> = T_0 + 1$ and $T_< = T_0 = (N-Z)/2$ (here, T_0 is the isospin of the ground state of the nucleus being considered), and on the ratio R of the intensities of GDR isospin components:

$$R = \sigma^>_{-1}/(\sigma^>_{-1} + \sigma^<_{-1}), \qquad (2)$$

where $\sigma_{-1} = \int \sigma E^{-1} dE$ is the first moment of the integrated GDR cross section.

For many nuclei (for example, for ^{14}C, ^{44,48}Ca, ^{48,54}Ti, ^{54}Cr, ^{54}Fe, ^{55}Cu, and ^{65}Co), experimental data exhibited significant deviations from the isospin-splitting values predicted by traditional theoretical models [2–5], which were proposed for relatively heavy ($A > 90$) nuclei. Specifically, the prediction has the form

$$\Delta E^{\mathrm{theor}} = U(T_0+1)/T_0 = U_0(T_0+1)/A, \qquad (3)$$

where $U = (U_0/A)T_0$, with U_0 being the nuclear-symmetry energy.

Several markedly different estimates are used in the literature for U_0. In particular, the value of $U_0 = 60$ MeV was obtained in [4] upon taking into account GDR coherent effects (the calculations were performed there for nuclei lighter than copper), while the value of $U_0 = 100$ MeV was found in [2] for single-particle excitations. The dependence $U_0(A)$ was calculated theoretically in [3], and it was found there that U_0 decreases with decreasing A: $U_0 \approx 60$ MeV in the region of large A, and $U_0 = 14$ MeV in the region of small A.

An expression for the ratio R was found in [2] on the basis a simple geometric model:

$$R^{\mathrm{theor}} = 1/(T_0+1). \qquad (4)$$

One can see that the intensity of the component $\sigma^>$ is less than the intensity of the component $\sigma^<$, the suppression factor being greater than the mere geometric-suppression factor ($1/T_0$), since the space of particle–hole excitations accessible to states of the component $\sigma^<$ of the GDR is much broader than that for states of the component $\sigma^>$.

On the basis of an analysis of a vast body of experimental data, it was shown in [1] that the above

*E-mail: Varlamov@depni.sinp.msu.ru

discrepancies reflect the individual character of manifestations of GDR isospin components in different nuclei. They are associated with the effect of energy and isospin constraints [6, 7] on the decay of isobar-analog states of such nuclei through the neutron channel. Such constraints are manifested in many experiments [8–12], but they are not taken into account within simple models.

The concept of the isospin splitting of the giant dipole resonance is essentially the following: in photon interaction with a nucleus whose ground-state isospin is $T_0 = (N - Z)/2 \neq 0$, two groups of levels characterized by the isospins $T_< = T_0$ and $T_> = T_0 + 1$ are excited in this nucleus. Such states are concentrated at different excitation energies: the $T_>$ states are higher than the $T_<$ states. Excited states having different isospin values have different decay channels. The decay of the $T_<$ states through channels involving neutron and proton emission is allowed. At the same time, the $T_>$ states decay predominantly via proton emission, since the emission of neutrons from them is not only energetically suppressed but also frequently forbidden by isospin-selection rules. As was shown in [13] and in many other studies, a significant change in the character of the energy dependence of the ratio of the cross sections for the corresponding reactions, $r = \sigma(\gamma,\ p)/\sigma(\gamma,\ n)$, is therefore a manifestation of the $T_>$ states against the background of the $T_<$ states. In the region dominated by the $T_<$ states, whose decay is symmetric with respect to the proton and neutron channels, the ratio r is expected to be close to some constant. As the $T_>$ states, which decay predominantly via proton emission, appear starting from some threshold and as their number grows with increasing excitation energy of the nucleus, the ratio r must increase.

In view of this, the following procedure was rather widely used earlier [6, 13–16] to study in detail the parameters of the isospin splitting of giant dipole resonances:

(i) From an analysis of the energy dependence of the ratio $r = \sigma(\gamma,\ p)/\sigma(\gamma,\ n)$, one determines the boundary photon-energy value at which a significant change in the character of this dependence from an approximate invariability to a substantial growth occurs.

(ii) In the energy regions below and above this boundary, the cross sections $\sigma(\gamma,\ p)$ and $\sigma(\gamma,\ n)$ are approximated by Gaussian functions in such a way that, in the low-energy region, the parameters of the Gaussian functions for the cross sections $\sigma(\gamma,\ p)$ and $\sigma(\gamma,\ n)$ were as close as possible (since the two cross sections in question are associated with the decay of the same nuclear states having the isospin $T_<$).

(iii) For the above cross sections, one determines the parameters of the $T_<$ components of giant dipole resonances from the Gaussian parameters in the low-energy region and the parameters of their $T_>$ components from the Gaussian parameters in the high-energy region.

(iv) One determines the isospin splitting ΔE in (1) from the spacing between the centroids of the sums of the corresponding components of the two cross sections in question and the ratio R in (2) from the respective integrated cross sections.

Table 1. Parameters of the isospin splitting in the ^{90}Zr nucleus [15]

Component	$T_<$	$T_>$
E_c [MeV]	16.7	20.4
$\sigma(\gamma,\ n)$ [mb]	211.0	29.0
$\sigma(\gamma,\ p)$ [mb]	23.5	26.0

The procedure outlined above and modified by approximating the experimental cross sections by Lorentzian rather than by Gaussian functions was used in [15, 16] to analyze data on the photodissociation of the ^{90}Zr nucleus—more precisely, the photoproton cross section from [15] and the photoneutron cross section from [17]. The resulting parameters of the isospin splitting in the ^{90}Zr nucleus are given in Table 1. According to the data from [15, 17], the isospin splitting in the ^{90}Zr nucleus is $\Delta E = 3.7$ MeV. The value obtained in [15] for the ratio of the components is $R = 0.1$ arbitrary units.

From the foregoing, it is clear that the estimates obtained in [15, 17] are plagued by a number of drawbacks:

(i) Data obtained in Saclay [17], which, because of the incorrectness of the procedure used there to determine the photoneutron multiplicity [18–22], require corrections, were taken for one of the reference cross sections—specifically, the $(\gamma,\ n)$ cross section.

(ii) The parameters of the isospin splitting of giant dipole resonances were estimated by using data only on the $(\gamma,\ p)$ and $(\gamma,\ n)$ channels without resort to data on the $(\gamma,\ np)$ and $(\gamma,\ 2n)$ channels, but relations (1) and (2) are associated with the total photoabsorption cross section rather than with cross sections for partial reactions.

(iii) The parameters of the isospin splitting of giant dipole resonances were estimated by using the absolute values of the amplitudes rather than the integrated features of reference reactions.

(iv) The cross sections were approximated by Lorentzian functions (which are more appropriate for describing the contributions of well-isolated slightly intersecting levels) rather than by Gaussian functions

(which are more appropriate for describing a resonance that combines several levels).

The present study is devoted to evaluating the parameters of the isospin splitting of the giant dipole resonance in the ^{90}Zr nucleus under conditions that make it possible to compensate for the above drawbacks to some extent. This is done by using the complete relational database of nuclear reactions induced by photons, neutrons, charged particles, and heavy ions [23] that was produced at the Centre for Photonuclear Experiments Data of the Skobeltsyn Institute of Nuclear Physics of Lomonosov Moscow State University.

2. SYSTEMATIC DISAGREEMENTS BETWEEN DATA FROM EXPERIMENTS WITH QUASIMONOCHROMATIC ANNIHILATION PHOTONS

The bulk of the data on $(\gamma,\ n)$ and $(\gamma,\ 2n)$ reactions were obtained in experiments with quasimonoenergetic annihilation photons in Livermore (USA) and Saclay (France) [24]. A detailed comparison of the results of those experiments was performed in [18, 19] for 12 nuclei (^{89}Y, ^{115}In, ^{117,118,120,124}Sn, ^{133}Cs, ^{159}Tb, ^{165}Ho, ^{181}Ta, ^{197}Au, and ^{208}Pb) and, later, in [22] for seven more nuclei (^{51}V, ^{75}As, ^{90}Zr, ^{116}Sn, ^{127}I, ^{232}Th, and ^{238}U).

The following results were obtained:

(i) The experimental cross sections directly determined in Saclay for $(\gamma,\ xn)$ total photoneutron reactions are larger in absolute value by about 6 to 16% than their counterparts obtained in Livermore. This complies with the total systematics from [21, 22], which covers a vast array of data from various laboratories on cross sections for the total photoneutron reactions

$$(\gamma,\ xn) = (\gamma,\ 1n) + (\gamma,\ np) + 2(\gamma,\ 2n) + 3(\gamma,\ 3n) + \ldots + \nu(\gamma,\ f). \quad (5)$$

According to this systematics, the average ratio of the integrated $(\gamma,\ xn)$ cross sections that were obtained in Saclay and Livermore is $\langle R\rangle = 1.12$ arbitrary units.

(ii) On the whole, the $(\gamma,\ n)$ cross sections obtained in Saclay are also (see Table 2) larger than the respective cross sections obtained in Livermore; however, their corresponding ratios are greatly in excess of the ratios of the $(\gamma,\ xn)$ cross sections—for example, the ratios of the integrated cross sections obtained for ^{89}Y, ^{127}I, and ^{208}Pb nuclei in Saclay and Livermore are 1.252, 1.336, and 1.212 arbitrary units, respectively, while this ratio for the ^{90}Zr nucleus, which is studied here, is 1.259 arbitrary units according to data from [22].

(iii) The ratios of the $(\gamma,\ 2n)$ cross sections show an opposite trend [22]—the ratios of the integrated cross sections obtained in Saclay and Livermore for the aforementioned nuclei are 0.874, 1.067, 0.771, and 0.728 arbitrary units, respectively.

The general systematics from [22] for the ratios of the cross sections determined in the two laboratories for the $(\gamma,\ n)$ and $(\gamma,\ 2n)$ partial reactions on 19 nuclei is presented in Fig. 1. It clearly illustrates the aforementioned oppositely directed discrepancies. The cross sections obtained in Saclay for the $(\gamma,\ n)$ reactions are as a rule larger than their Livermore counterparts (the boxes lie in the region above unity), but the hierarchy of the $(\gamma,\ 2n)$ cross sections is inverse (the triangles fall within the region of values below unity). Three "special" cases (triangles in the region above unity) and two "ideal" cases (triangles and boxes close to each other and to unity) were examined in [22] individually.

In [18–22], it was shown that the incorrectness of the special procedure used in the Saclay experiments to sort photoneutrons in multiplicity is the reason behind the observed discrepancies. In the GDR energy region considered here (which extends up to 26 MeV), the relevant $(\gamma,\ n)$ and $(\gamma,\ 2n)$ reactions, whose contributions to the cross section for the total photoneutron reaction (5) were determined by means of this sorting procedure (appearance of one versus two neutrons in the reaction was established), are related by the equation

$$\sigma(\gamma,\ xn) = \sigma(\gamma,\ n) + 2\sigma(\gamma,\ 2n). \quad (6)$$

Because of this, a determination of the cross sections for one of these reactions with a large systematic error inevitably leads to a significant systematic error in the cross section for the other reaction: an underestimation (overestimation) of the absolute value of the $(\gamma,\ n)$ cross section leads to an overestimation (underestimation) of the absolute value of the $(\gamma,\ 2n)$ cross section. It is obvious that, without a detailed analysis of the reasons behind the aforementioned systematic discrepancies and without the development of an efficient method for their elimination, a simultaneous use of the experimental data being discussed is open to criticism.

In [19, 22], the reasons behind the systematic discrepancies under discussion were analyzed for almost all of the aforementioned nuclei, which were studied in both the Livermore and Saclay laboratories. A method for removing these discrepancies was developed, and mutually corrected cross sections for total and partial photoneutron reactions were evaluated for all nuclei considered there. Not only did the results prove to be self-consistent, but they also complied well with cross sections obtained in experiments of different types—first of all, in experiments with beams of bremsstrahlung photons.

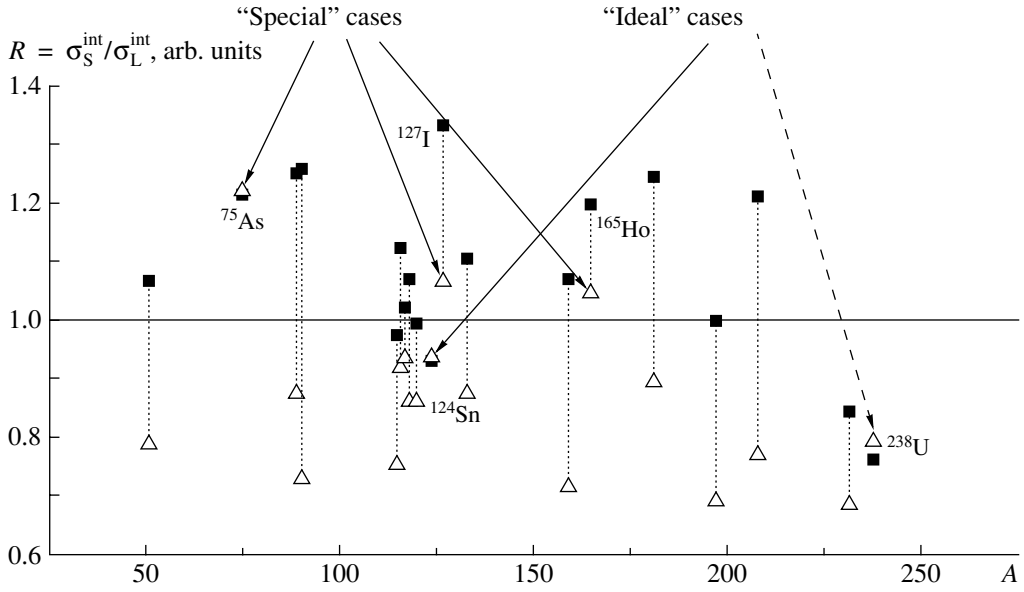

Fig. 1. Systematics of the ratios $R(n) = \sigma_S^{int}(\gamma, n)/\sigma_L^{int}(\gamma, n)$ (closed boxes, which basically lie in the region above 1.0) and $R(2n) = \sigma_S^{int}(\gamma, 2n)/\sigma_L^{int}(\gamma, 2n)$ (open triangles, which basically lie in the region below 1.0) from [22] that were obtained for matched domains of integration on the basis of data from experiments performed in Saclay and Livermore. "Special" (open triangles in the region above 1.0) and "ideal" (open triangles and closed boxes are close to each other and to 1.0) cases were considered in [22] individually.

3. CORRECTION OF DATA ON CROSS SECTIONS FOR (γ, n) AND $(\gamma, 2n)$ REACTIONS

3.1. Special Features of the Procedure for Determining the Neutron Multiplicity in Experiments with Quasimonoenergetic Annihilation Photons

The aforementioned total systematics [21] of data on the cross sections for the total photoneutron reactions (5) was constructed on the basis of reaction cross sections calculated in the energy regions below the threshold for $(\gamma, 2n)$ reactions, where it was unnecessary to take into account reactions involving large photoneutron multiplicities. At high energies, where there arise conditions for the production of different numbers of photoneutrons, the character of the discrepancies between the Saclay and Livermore data becomes totally different (see Table 2 and Fig. 1) and much more intricate. Methods for taking into account and removing such discrepancies were considered individually in [18, 19, 22] with allowance for information about the procedures for determining multiplicities in photoneutron reactions.

3.1.1. Method of ring ratios (Livermore). The problem of separating the contributions from (γ, n) and $(\gamma, 2n)$ reactions was solved in Livermore by means of a highly efficient neutron detector constructed in such a way as to provide the possibility of recording moderated photoneutrons with the aid of BF_3 counters arranged at different distances from the target in the form of concentric rings around it. The ratio of the numbers of counts in the inner and outer rings grows monotonically with increasing mean energy of photoneutrons. With the aid of the technique of ring ratios, the mean neutron energies and, accordingly, the ratios for events of reactions featuring one and two neutrons are determined independently. This permits quite reliably separating, by using data on the detection efficiency for neutrons of different energy, cross sections for partial reactions characterized by different multiplicities.

3.1.2. Method of calibration of the energy dependence of the neutron-detector efficiency (Saclay). A method based on a precision calibration of a large-volume liquid scintillator (including gadolinium in its composition) with the aid of a ^{252}Cf source was used in Saclay. Although the neutron-energy dependence of the detector efficiency is not in fact a constant within any segment, it was assumed that the deviations of the detection efficiency from a constant are sizable only for neutrons of energy $E_n \sim 5$ MeV, with photoneutron energy in the giant-dipole-resonance region not being in excess of $E_n \sim 3$ MeV. This assumption is not well justified since it is well known that the energy of photoneutrons from (γ, n) and $(\gamma, 2n)$ reactions may be as high as about 10 MeV. Moreover, information reported thus far on this procedure indicates that the detector efficiency determined with the aid of a ^{252}Cf source was close

Table 2. Basic data used in a comparison of the ratio of the integrated cross sections obtained in Saclay and Livermore [$E^{\rm int}_{\rm min}$ and $E^{\rm int}_{\rm max}$ are, respectively, the lower and the upper limit of integration of $(\gamma, 2n)$ cross sections]

Nucleus	Reaction threshold for $(\gamma,\ 2n)$, MeV	$R(n) = \sigma^{\rm int}_{\rm S}(\gamma,\ n)/\sigma^{\rm int}_{\rm L}(\gamma,\ n)$, arb. units	$E^{\rm int}_{\rm min}$, MeV	$E^{\rm int}_{\rm max}$, MeV	$R(2n) = \sigma^{\rm int}_{\rm S}(\gamma,\ 2n)/\sigma^{\rm int}_{\rm L}(\gamma,\ 2n)$, arb. units
$^{51}_{23}$V	20.4	1.066	20.4	27.78	0.788
$^{75}_{33}$As	18.2	1.214	18.2	26.2	1.223
$^{89}_{39}$Y	20.8	1.252	21.03	27.02	0.874
$^{90}_{40}$Zr	21.3	1.259	21.57	25.93	0.728
$^{115}_{49}$In	16.3	0.974	16.46	24.05	0.756
$^{116}_{50}$Sn	17.1	1.103	17.1	22.12	0.919
$^{117}_{50}$Sn	16.5	1.022	16.73	21.06	0.934
$^{118}_{50}$Sn	16.3	1.071	16.3	21.57	0.861
$^{120}_{50}$Sn	15.6	0.995	15.6	22.39	0.862
$^{124}_{50}$Sn	14.4	0.932	14.56	21.61	0.936
$^{127}_{53}$I	16.3	1.336	16.3	29.54	1.067
$^{133}_{55}$Cs	16.2	1.104	16.2	24.16	0.875
$^{159}_{65}$Tb	14.9	1.071	14.9	27.99	0.714
$^{165}_{67}$Ho	14.7	1.2	14.7	28.48	1.049
$^{181}_{73}$Ta	14.2	1.247	14.2	24.58	0.894
$^{197}_{79}$Au	14.7	0.999	14.7	24.70	0.691
$^{208}_{82}$Pb	14.1	1.212	14.1	26.33	0.771
$^{232}_{90}$Th	11.6	0.844	11.6	16.33	0.685
$^{238}_{92}$U	11.3	0.762	11.3	18.26	0.793

to unity, but that, in real experiments, the detecting system was used under time conditions such that this efficiency was as low as about 0.6. A rather high background level in the detector and a signal-to-noise ratio much poorer than that in Livermore were an obvious and quite significant drawback of the procedure used in Saclay to determine photoneutron multiplicities. These factors complicated the separation and subtraction of this background and the introduction of corrections for random coincidences in the actuation of the counters. All this could lead to overestimating the fraction of events of $(\gamma,\ n)$ single-neutron reactions in relation to events of reactions involving the emission of two (as well as three or more) neutrons.

On the basis of the aforesaid, we can conclude that, although the efficiency of the detector in Livermore was somewhat lower than the efficiency of the detector in Saclay, the ring-ratio method used in Livermore compensated for this drawback to a considerable extent. Thus, it should be noted that the multiplicities in photoneutron reactions were determined by substantially different methods in Livermore and in Saclay. Of course, the question of which procedure is more correct (or, on the contrary, erroneous) is of particular interest.

In [19], data obtained for the ^{181}Ta nucleus in Saclay and Livermore were analyzed along with the results of the investigations performed in [25–27] for the $(e,\ xn)$, $(e,\ n)$, and $(e,\ 2n)$ reactions on this nucleus. Since the cross sections for the electro- and photodisintegration of nuclei can be related [26, 27] to each other by using the spectrum of virtual photons, it is possible to evaluate the $(e,\ 2n)$ cross section on the basis of data on the respective $(\gamma,\ 2n)$ reaction. The experimental cross section for the reaction ^{181}Ta$(e,\ 2n)$ was obtained in [25] by means of the obvious relation

$$\sigma(e,\ 2n) = \tfrac{1}{2}(\sigma(e,\ xn) - \sigma(e,\ n)), \qquad (7)$$

where use was made of the experimentally determined values of the cross sections $\sigma(e,\ xn)$ and $\sigma(e,\ n)$.

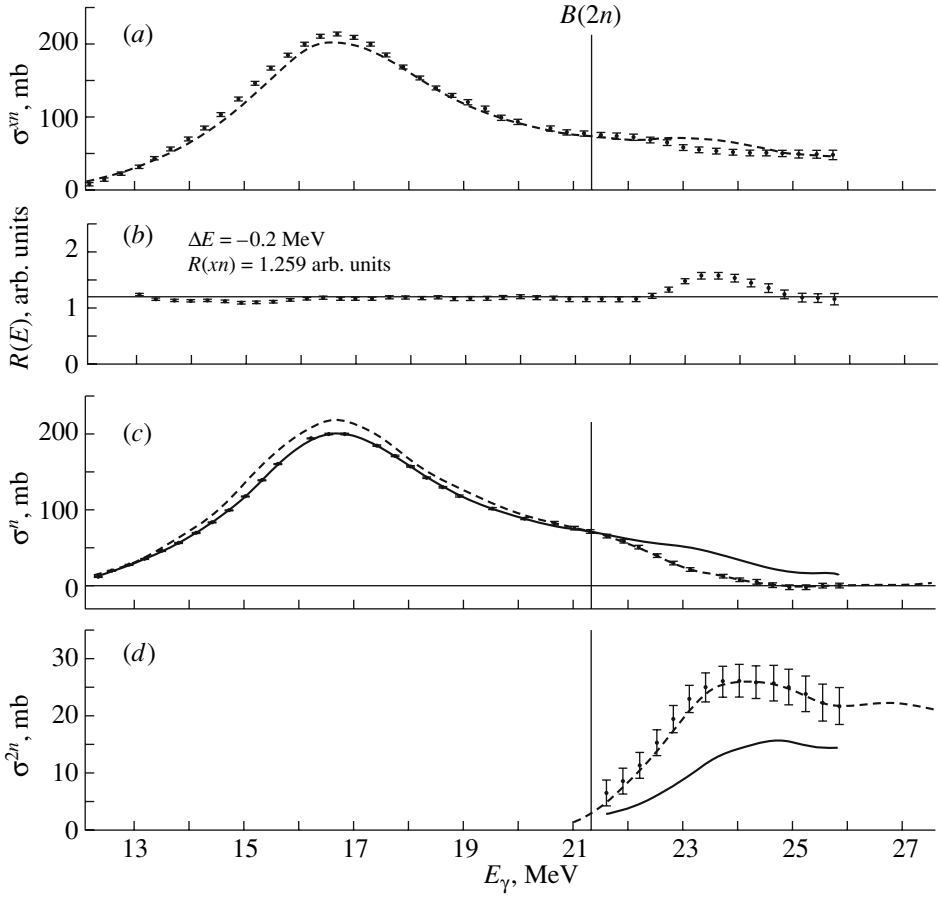

Fig. 2. Results obtained by mutually correcting ("special" case) the reaction cross sections obtained in Saclay and Livermore for the ^{90}Zr nucleus: (*a*) Saclay data on $(\gamma,\ xn)$ cross sections [(dashed curve) original values of σ_S^{xn} and (points with error bars) corrected values of $\sigma_S^{xn*} = \sigma_S^{xn} R/R(E)$], (*b*) ratios $R(E)$ of $(\gamma,\ xn)$ cross sections [the values of ΔE and $R(xn)$ are indicated], (*c*) data on $(\gamma,\ n)$ cross sections [(solid curve) original Saclay values of σ_S^n, (points with error bars) Saclay values of σ_S^{n*} as estimated with the aid of (12), and (dashed curve) estimated Livermore values of $R\sigma_L^n$], and (*d*) data on $(\gamma,\ 2n)$ cross sections [(solid curve) original Saclay values of σ_S^{2n}, (points with error bars) Saclay values of σ_S^{2n*} as estimated with the aid of (9)–(11), and (dashed curve) estimated Livermore values of $R\sigma_L^{2n}$].

The cross section $\sigma(e,\ n)$, which appears in (7), was measured two times: as $\sigma_1(e,\ n)$ found by a method that involves determining the neutron multiplicity and as $\sigma_2(e,\ n)$ found by the induced-activity method [the 93.3-keV γ line associated with the nuclear-decay process $^{180}\mathrm{Ta} \to {}^{180}\mathrm{Hf}$ ($T_{1/2} = 8.15$ h) was recorded in experiments with a GeLi detector]. The value of $\langle \sigma_1(e,\ n)/\sigma_2(e,\ n) \rangle = 1.057 \pm 0.023$ was obtained for the weighted-mean ratio of the measured cross sections. The proximity of this ratio to unity indicates that the procedure used to determine photoneutron-reaction multiplicities is quite reliable. It was found that the cross section $\sigma(e,\ 2n)$ (7) is in agreement with data rescaled from Livermore data on $(\gamma,\ 2n)$, but that it is at odds with the corresponding Saclay data, which are underestimated for $(\gamma,\ 2n)$ cross sections and, on the contrary, are overestimated for $(\gamma,\ n)$ cross sections.

3.2. Mutual Correction of Data on the Cross Sections for $(\gamma,\ n)$ and $(\gamma,\ 2n)$ Partial Photoneutron Reactions

From the aforesaid, it is clear that mutual correction is necessary in order to remove the above discrepancies between the data obtained in Scalay and in Livermore for the $(\gamma,\ n)$ and $(\gamma,\ 2n)$ cross sections and in order to match them with each other. The results of the investigations performed in [18, 19, 22] indicate that, since the data obtained in Saclay and Livermore show substantially different discrepancies in the energy regions below and above the energy thresholds for $(\gamma,\ 2n)$ reactions, the respective correction method must take into account the flaws revealed in the procedure used in Saclay to determine photoneutron-reaction multiplicities.

3.2.1. Estimating $(\gamma,\ 2n)$ cross sections. On the basis of the investigations performed in [18, 19,

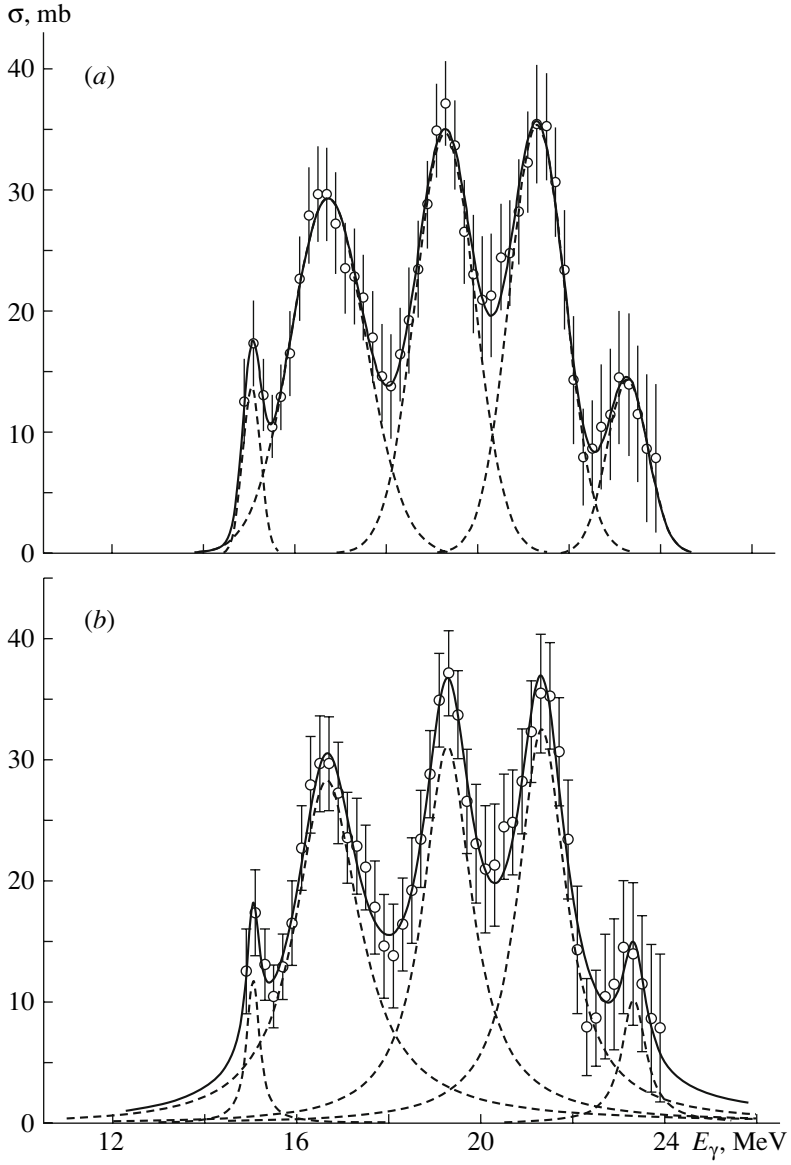

Fig. 3. Approximations of the energy dependence (dashed curves) of the cross section for the reaction ^{90}Zr(γ, p) [15, 16] by (*a*) five Gaussian functions (Table 3, left column) and (*b*) five Lorentzian functions (Table 3, right column).

22], the discrepancies between the Saclay and Livermore data are interpreted as manifestations of the errors in the procedure used in Saclay to determine photoneutron-reaction multiplicities [some neutrons from (γ, $2n$) reactions are misidentified as those from (γ, n) reactions]. The essence of the method for taking into account the discrepancies is that data obtained for (γ, $2n$) cross sections in Saclay, where the photoneutron multiplicity was determined with large errors, are rescaled, and part of the (γ, n) cross section erroneously associated with processes of single-neutron production is given back to the cross section for the respective two-neutron reaction.

This rescaling was implemented in the following way:

(i) After the required correction of the energy scales of the cross sections under comparison according to data on the cross sections directly measured in the experiments for the (γ, xn) total photoneutron reactions [shift of the cross sections obtained in Livermore along the energy scale by some value ΔE (Fig. 2) to the Saclay data], one determines the coefficient

$$R = R(xn) = \sigma_{\mathrm{S}}^{\mathrm{int}}(\gamma,\ xn)/\sigma_{\mathrm{L}}^{\mathrm{int}}(\gamma,\ xn), \qquad (8)$$

which normalizes the cross sections for total photoneutron reactions in the energy region below the threshold $B(2n)$ for (γ, $2n$) reactions, where they must be identical in the two laboratories.

(ii) By virtue of relation (6), the use of the coeffi-

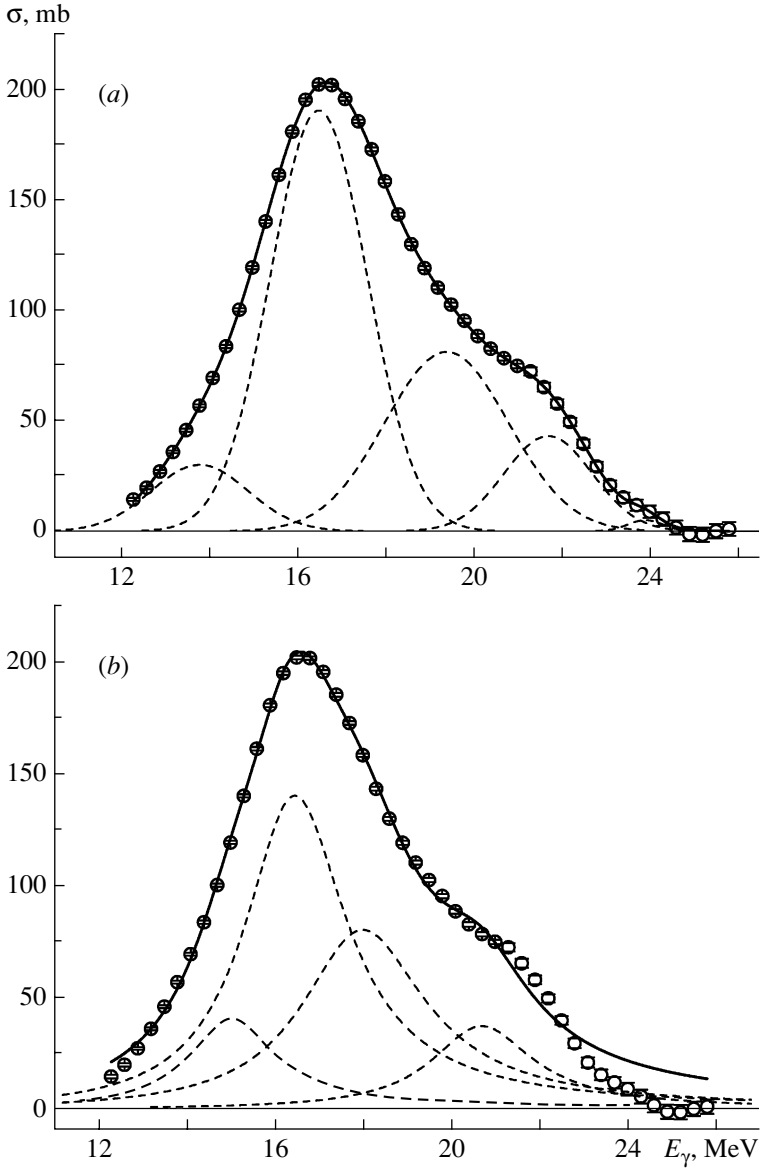

Fig. 4. Approximations of the energy dependence (dashed curves) of the cross section for the reaction ^{90}Zr$(\gamma,\ n)$ [21, 22] by (*a*) five Gaussian functions (Table 4, left column) and (*b*) four Lorentzian functions (Table 4, right column).

cient R makes it possible to obtain an expression that is employed for the aforementioned restitution of part of the $(\gamma,\ n)$ cross section obtained in Saclay to the new (corrected) $(\gamma,\ 2n)$ cross section:

$$R = \sigma_{\rm S}^{xn}/\sigma_{\rm L}^{xn} = (\sigma_{\rm S}^{n} + 2\sigma_{\rm S}^{2n})/(\sigma_{\rm L}^{n} + 2\sigma_{\rm L}^{2n}), \quad (9)$$

$$\sigma_{\rm S}^{xn} = (\sigma_{\rm S}^{n} + 2\sigma_{\rm S}^{2n}) = R\sigma_{\rm L}^{xn} = R(\sigma_{\rm L}^{n} + 2\sigma_{\rm L}^{2n}), \quad (10)$$

$$R\sigma_{\rm L}^{2n} = \sigma_{\rm S}^{2n*} = \sigma_{\rm S}^{2n} + \tfrac{1}{2}(\sigma_{\rm S}^{n} - R\sigma_{\rm L}^{n}). \quad (11)$$

The right-hand side of the basic relation (11) in the method for correcting data obtained in Saclay on $(\gamma,\ 2n)$ cross sections has the meaning discussed above: to the value $\sigma_{\rm S}^{2n}$ obtained in Saclay for the $(\gamma,\ 2n)$ cross section, one adds that part $\frac{1}{2}(\sigma_{\rm S}^{n} - R\sigma_{\rm L}^{n})$ of the $(\gamma,\ n)$ cross section which was calculated with allowance for the coefficient R (8). If the discrepancy between the Livermore and Saclay data is due exclusively to the errors in the procedure used in Saclay to determine photoneutron-reaction multiplicities, then, according to the left-hand side of relation (11), the rescaled Saclay cross section $\sigma_{\rm S}^{2n*}$ must agree with the Livermore cross section $\sigma_{\rm L}^{2n}$ multiplied by the coefficient R (8): $\sigma_{\rm L}^{2n*} = R\sigma_{\rm L}^{2n}$.

The corrected Saclay cross sections $\sigma_{\rm S}^{2n*}$, together with the original cross sections from [17] and the corrected Livermore cross sections $\sigma_{\rm L}^{2n*}$, are given

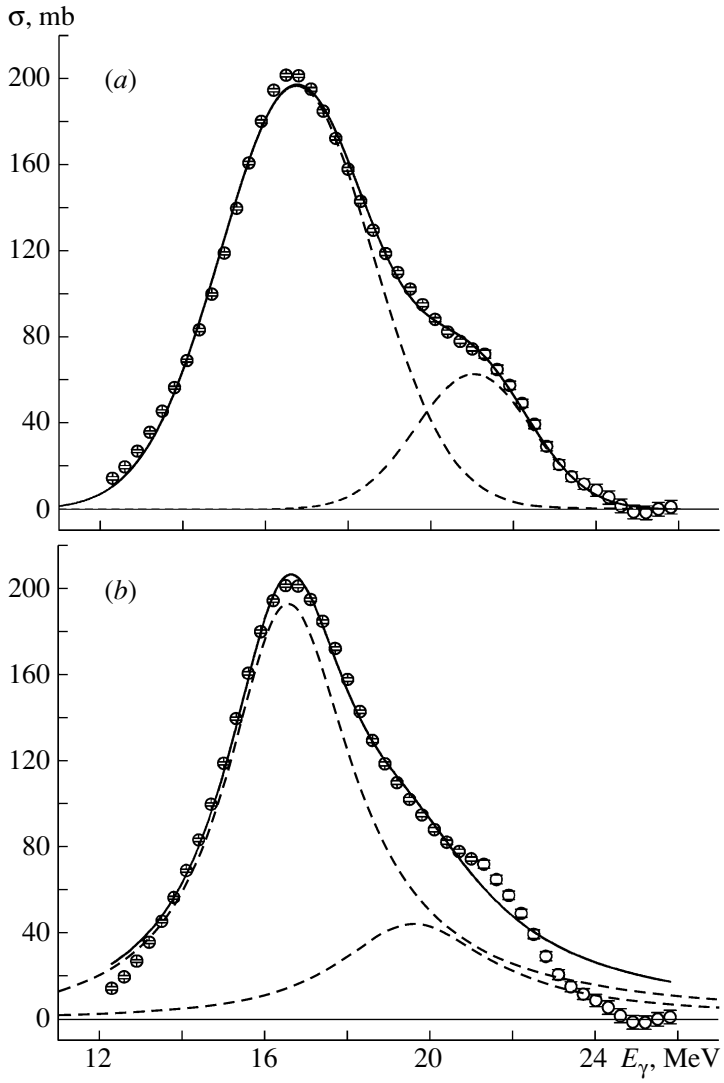

Fig. 5. Approximations of the energy dependence (dashed curves) of the cross section for the reaction ^{90}Zr$(\gamma,\ n)$ [21, 22] by (a) two Gaussian functions and (b) two Lorentzian functions.

in [22] for the 19 aforementioned nuclei. For the ^{90}Zr nucleus, these data are displayed in Fig. 2d. One can see that, within the errors, the mutually corrected data agree with each other.

3.2.2. Estimating $(\gamma,\ n)$ cross sections. Since the essence of the applied correction method [19, 22] consists in giving back, to the $(\gamma,\ 2n)$ cross section, its part earlier erroneously associated with the $(\gamma,\ n)$ reactions, the $(\gamma,\ n)$ cross sections obtained in Saclay [17] can also be corrected [22]. For this, one must remove, from the $(\gamma,\ n)$ cross section, its part that is included [see Eq. (11)] in the $(\gamma,\ 2n)$ cross section. The corrected $(\gamma,\ n)$ cross section [22] must have the form

$$R\sigma_{\rm L}^{n} = \sigma_{\rm L}^{n*} = \sigma_{\rm S}^{n*} = \sigma_{\rm S}^{n} - (\sigma_{\rm S}^{n} - R\sigma_{\rm L}^{n}), \qquad (12)$$

where the difference $(\sigma_{\rm S}^{n} - R\sigma_{\rm L}^{n})$ is calculated in the energy region above $B(2n)$.

The corrected Saclay cross sections $\sigma_{\rm S}^{n*}$ for the same ^{90}Zr nucleus are given in Fig. 2c together with the respective original cross sections and the respective corrected Livermore cross sections $\sigma_{\rm L}^{n*} = R\sigma_{\rm L}^{n}$.

From Table 2 and from Fig. 2, one can see that the data used previously in [15, 16] for the cross sections for the reactions ^{90}Zr$(\gamma,\ n)^{89}$Zr and ^{90}Zr$(\gamma,\ 2n)^{88}$Zr to determine the parameters of the isospin splitting of the giant dipole resonance in the ^{90}Zr nucleus required a significant correction. In the present study, the corrected cross sections for photoneutron reactions from [22] and the cross section for the reaction ^{90}Zr$(\gamma,\ p)^{89}$Y from [15] are used for a new evaluation

Table 3. Parameters of the approximation of the ^{90}Zr(γ, p) cross sections

Five Gaussian functions (13)	Five Lorentzian functions (14)
$\chi^2 = 0.177$	$\chi^2 = 0.227$
$A_1^{\max} = 14.0 \pm 4.0$ mb $E_1^{\max} = 15.1 \pm 0.1$ MeV $\sigma_1^G = 0.2 \pm 0.1$ MeV $\Gamma_1 = 0.5 \pm 0.2$ MeV	$A_1^{\max} = 11.7 \pm 4.4$ mb $E_1^{\max} = 15.1 \pm 0.1$ MeV $\Gamma_1 = 0.3 \pm 0.2$ MeV
$A_2^{\max} = 29.0 \pm 2.0$ mb $E_2^{\max} = 16.7 \pm 0.1$ MeV $\sigma_2^G = 0.8 \pm 0.1$ MeV $\Gamma_2 = 1.9 \pm 0.2$ MeV	$A_2^{\max} = 28.3 \pm 2.2$ mb $E_2^{\max} = 16.7 \pm 0.1$ MeV $\Gamma_2 = 1.7 \pm 0.3$ MeV
$A_3^{\max} = 35.0 \pm 2.0$ mb $E_3^{\max} = 19.3 \pm 0.1$ MeV $\sigma_3^G = 0.7 \pm 0.1$ MeV $\Gamma_3 = 1.5 \pm 0.3$ MeV	$A_3^{\max} = 31.1 \pm 2.4$ mb $E_3^{\max} = 19.3 \pm 0.1$ MeV $\Gamma_3 = 1.3 \pm 0.2$ MeV
$A_4^{\max} = 35.0 \pm 2.0$ mb $E_4^{\max} = 21.3 \pm 0.1$ MeV $\sigma_4^G = 0.6 \pm 0.1$ MeV $\Gamma_4 = 1.4 \pm 0.2$ MeV	$A_4^{\max} = 32.4 \pm 3.0$ mb $E_4^{\max} = 21.3 \pm 0.1$ MeV $\Gamma_4 = 1.3 \pm 0.2$ MeV
$A_5^{\max} = 14.0 \pm 4.0$ mb $E_5^{\max} = 23.3 \pm 0.1$ MeV $\sigma_5^G = 0.5 \pm 0.1$ MeV $\Gamma_5 = 1.1 \pm 0.4$ MeV	$A_5^{\max} = 10.2 \pm 5.3$ mb $E_5^{\max} = 23.3 \pm 0.2$ MeV $\Gamma_5 = 0.6 \pm 0.5$ MeV

Table 4. Parameters of the approximation of the ^{90}Zr(γ, n) cross section

Five Gaussian functions (13)	Four Lorentzian functions (14)
$\chi^2 = 0.458$	$\chi^2 = 16.6$
$A_1^{\max} = 30.0 \pm 4.0$ mb $E_1^{\max} = 13.8 \pm 0.1$ MeV $\sigma_1^G = 1.1 \pm 0.1$ MeV $\Gamma_1 = 2.6 \pm 0.2$ MeV	$A_1^{\max} = 30.0 \pm 10.0$ mb $E_1^{\max} = 14.9 \pm 0.1$ MeV $\Gamma_1 = 2.3 \pm 0.3$ MeV
$A_2^{\max} = 190.0 \pm 1.0$ mb $E_2^{\max} = 16.5 \pm 0.1$ MeV $\sigma_2^G = 1.1 \pm 0.1$ MeV $\Gamma_2 = 3.2 \pm 0.1$ MeV	$A_2^{\max} = 130.0 \pm 30.0$ mb $E_2^{\max} = 16.3 \pm 0.1$ MeV $\Gamma_2 = 2.6 \pm 0.4$ MeV
$A_3^{\max} = 81.0 \pm 1.0$ mb $E_3^{\max} = 19.4 \pm 0.2$ MeV $\sigma_3^G = 1.4 \pm 0.1$ MeV $\Gamma_3 = 3.3 \pm 0.3$ MeV	$A_3^{\max} = 100.0 \pm 20.0$ mb $E_3^{\max} = 17.7 \pm 0.1$ MeV $\Gamma_3 = 3.3 \pm 0.4$ MeV
$A_4^{\max} = 43.0 \pm 9.0$ mb $E_4^{\max} = 21.7 \pm 0.2$ MeV $\sigma_4^G = 1.0 \pm 0.1$ MeV $\Gamma_4 = 2.4 \pm 0.2$ MeV	$A_4^{\max} = 42.0 \pm 4.0$ mb $E_4^{\max} = 20.5 \pm 0.1$ MeV $\Gamma_4 = 3.4 \pm 0.3$ MeV
$A_5^{\max} = 5.0 \pm 2.0$ mb $E_5^{\max} = 23.9 \pm 0.2$ MeV $\sigma_5^G = 0.4 \pm 0.2$ MeV $\Gamma_5 = 0.9 \pm 0.5$ MeV	Absent

of the parameters of the isospin splitting of the giant dipole resonance in this nucleus.

4. DETERMINATION OF THE PARAMETERS OF THE ISOSPIN SPLITTING OF THE GIANT DIPOLE RESONANCE ON THE BASIS OF DATA ON PHOTONEUTRON AND PHOTOPROTON REACTIONS

4.1. Analysis of the Energy Dependence of the Cross Sections for the Reactions $^{90}Zr(\gamma, p)^{89}Y$ and $^{90}Zr(\gamma, n)^{89}Zr$

Investigations performed previously (see, for example, [7, 10, 15]) revealed that, since, according to the concept of isospin splitting [2–5], $T_>$ states decay predominantly via proton emission, a significant change in the character of the energy dependence of the ratio $r = \sigma(\gamma, p)/\sigma(\gamma, n)$ in favor of protons would be a manifestation of isospin-$T_>$ states against the background of isospin-$T_<$ states. The cross section for the photoproton reaction from [15] and the corrected cross sections for the photoneutron reactions on the ^{90}Zr nucleus from [22] were used to determine the ratio r. These cross sections are given in Figs. 3 and 4, respectively.

The energy dependence of the ratio r as estimated on the basis of the reaction cross sections preliminarily smoothed with the aid of Gaussian distributions that have a width of 2 MeV is shown in Fig. 6. One can clearly see that the cross-section ratio r remains approximately invariable over the excitation-energy region below $E_\gamma \approx 17.7$ MeV. This suggests that the states of the ^{90}Zr nucleus that are excited in this region decay through the proton and neutron channels with approximately identical probabilities. At higher energies, the cross-section ratio r begins growing rather quickly, which is indicative of the increasing role of levels of the ^{90}Zr nucleus—they decay predominantly through the proton (rather than through the neutron) channel.

With allowance for the aforesaid and on the basis of data in Fig. 5, it would be reasonable to assume that the formation and decay of states of the giant dipole resonance in the ^{90}Zr nucleus proceeds in such a way that its $T_<$ states are concentrated predominantly at excitation energies below $E_\gamma \approx 17.7$ MeV, while its $T_>$ states are concentrated at higher energies. Thus, the problem of determining the parameters of the isospin splitting of the giant dipole resonance can be solved by approximating the corre-

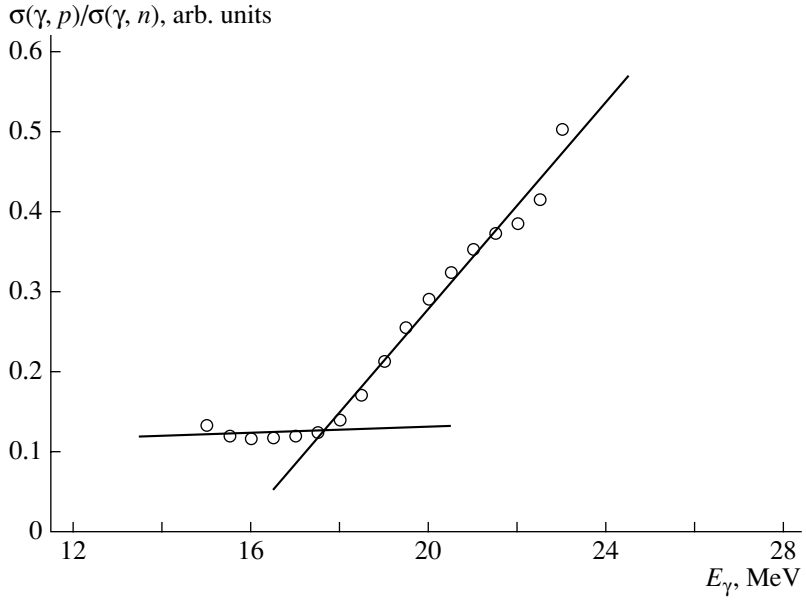

Fig. 6. Ratio $r = \sigma(\gamma,\ p)/\sigma(\gamma,\ n)$ of the cross sections for the $(\gamma,\ p)$ and $(\gamma,\ n)$ reactions on the ^{90}Zr nucleus as a function of energy (both cross sections were preliminarily smoothed by using a Gaussian distribution of width 2 MeV). The straight lines illustrate the presence of a break at an energy of 17.7 MeV.

sponding $T_<$ and $T_>$ components of the giant dipole resonance.

4.2. Approximation of Cross Section for the Reactions $^{90}Zr(\gamma,\ p)^{89}Y$ and $^{90}Zr(\gamma,\ n)^{89}Zr$

Cross section for the reaction ^{90}Zr(γ, p)^{89}Y. The experimental photoproton cross section for the ^{90}Zr nucleus [15, 16] (Fig. 3) displays five overlapping resonances. In view of this, it is reasonable to approximate this cross section by five resonance curves rather than by a single resonance curve (or two such curves that could correspond to two isospin components). In order to explore the possible effect of taking into account the overlap of these resonances, we compared an approximation by Gaussian functions [see Eq. (13) below], which are usually used to describe overlapping resonances, and an approximation by Lorentzian functions [see Eq. (14) below], which are usually used to describe individual resonances:

$$G(E_\gamma) = A\exp\left(-\frac{(E_\gamma - E_{\max})^2}{2\sigma^2}\right), \qquad (13)$$

$$L(E_\gamma) = \frac{A}{1+\left(\dfrac{E_\gamma^2 - E_{\max}^2}{E_\gamma\Gamma}\right)^2}. \qquad (14)$$

The main parameters of the best versions of these approximations are given in, respectively, the left and the right column of Table 3. They specify approximations characterized by markedly different but moderately small (in either case) values of χ^2, $\chi^2 = 0.177$ and 0.227.

Cross section for the reaction ^{90}Zr(γ, n)^{89}Zr. Although the structure of this cross section is not as pronounced as in the preceding case, its shape is similar (see Fig. 4).

As before, the approximation by five Gaussian functions (13) leads to (Table 4, left column) the smallest value of χ^2, $\chi^2 = 0.458$. In the case of approximations by four, three, or two Gaussian functions, the agreement with the experimental cross section deteriorates substantially: $\chi^2 = 0.53$, 2.39, or 18.88, respectively.

It should be emphasized that the positions of the maxima of the corresponding Gaussian distributions on the energy scale that were used to approximate the photoproton (Table 3, left column) and the photoneutron (Table 4, left column) cross section, with the exception of the positions of the first (the most low-energy) ones, are rather close to each other: 16.7 versus 16.5 MeV, 19.3 versus 19.4 MeV, 21.3 versus 21.7 MeV, and 23.3 versus 23.9 MeV. This seems quite natural since the same excited states of the ^{90}Zr nucleus decay through the two nucleon channels, that which involves proton emission and that which involves neutron emission. At the same time, a sizable distinction (15.1 versus 13.8 MeV) between the positions of the first (most low-energy) Gaussian distributions also has a natural explanation: the presence

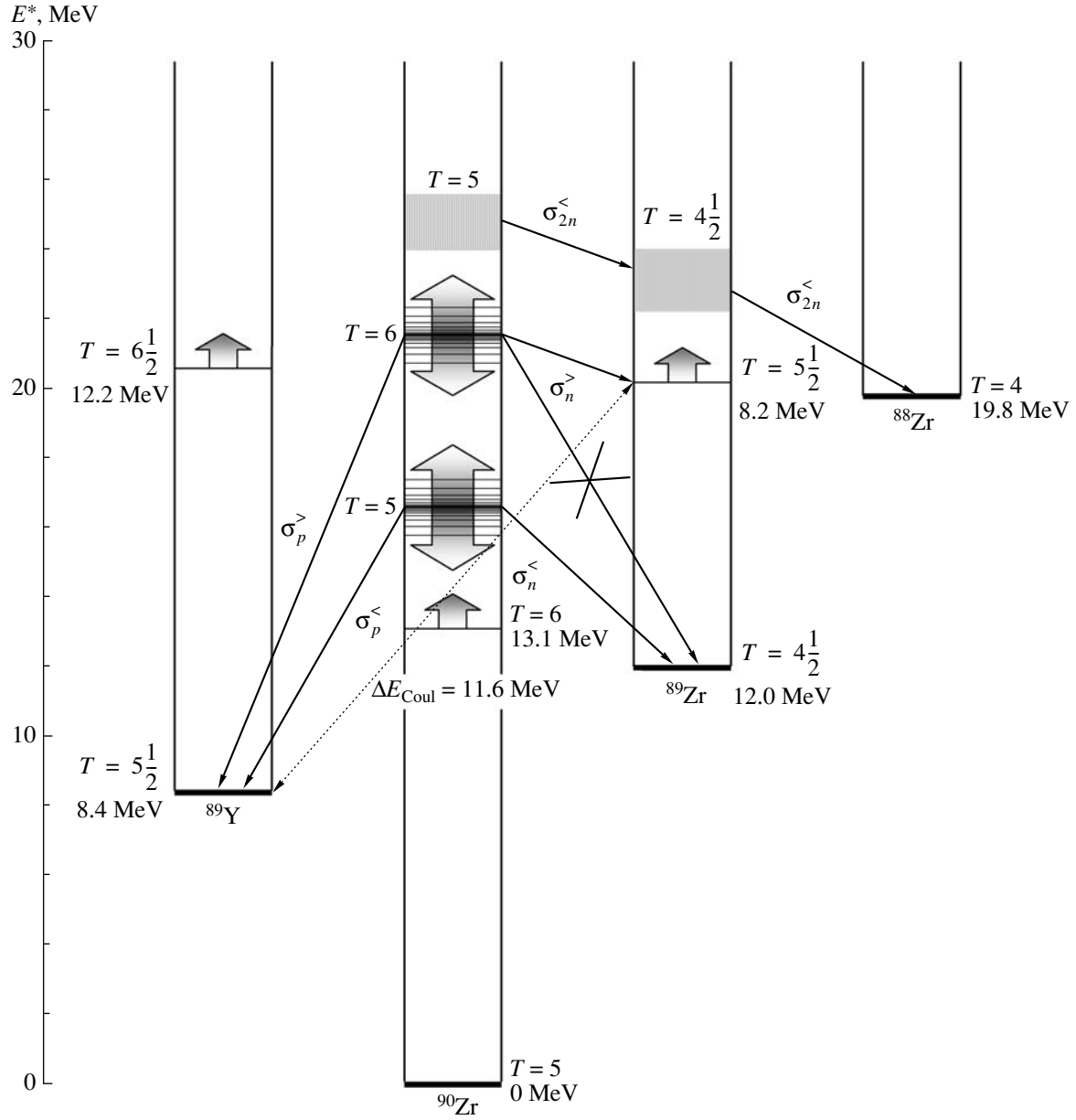

Fig. 7. Scheme of the excitation and decay of different-isospin levels in the ^{90}Zr nucleus and nuclei neighboring it. Shown in the figure (dotted-line arrow) is the shift of the lowest isospin-5/2 level in the ^{89}Zr nucleus by the Coulomb energy of $\Delta E_{\mathrm{Coul}} = 1.444(Z - 1/2)A^{-1/3} - 1.131 = 11.6$ MeV with respect to the ground-state of the ^{89}Y nucleus (the ^{89}Zr and ^{89}Y nuclei are members of the corresponding isospin multiplet). Also, the positions on the energy scale [28] of the first levels whose isospin is higher by unity than the ground-state isospin are presented for these nuclei (wide arrows).

of an energy threshold for proton detection leads to the loss of some of the most low-energy protons and, hence, to a shift of the corresponding maximum in the photoproton cross section toward higher energies.

In the case of an approximation by Lorentzian functions (14), the smallest (albeit a large one as it is) value of $\chi^2 = 16.6$ is attained for the case of four curves (Table 4, right column). This is because the relatively weak fifth maximum, which is situated at an energy of about 23 MeV, is lost against the background of the high-energy tails of the resonances occurring at lower energies. Concurrently, the positions on the energy scale of the corresponding Lorentzian functions representing the photoproton (Table 3, right column) and the photoneutron (Table 4, right column) cross section differ significantly, especially in the region of high energies. Specifically, we have 15.1 versus 14.9 MeV, 16.7 versus 16.3 MeV, 19.3 versus 17.7 MeV, and 21.3 versus 20.5 MeV. All flaws in the procedure based on employing Lorentzian functions

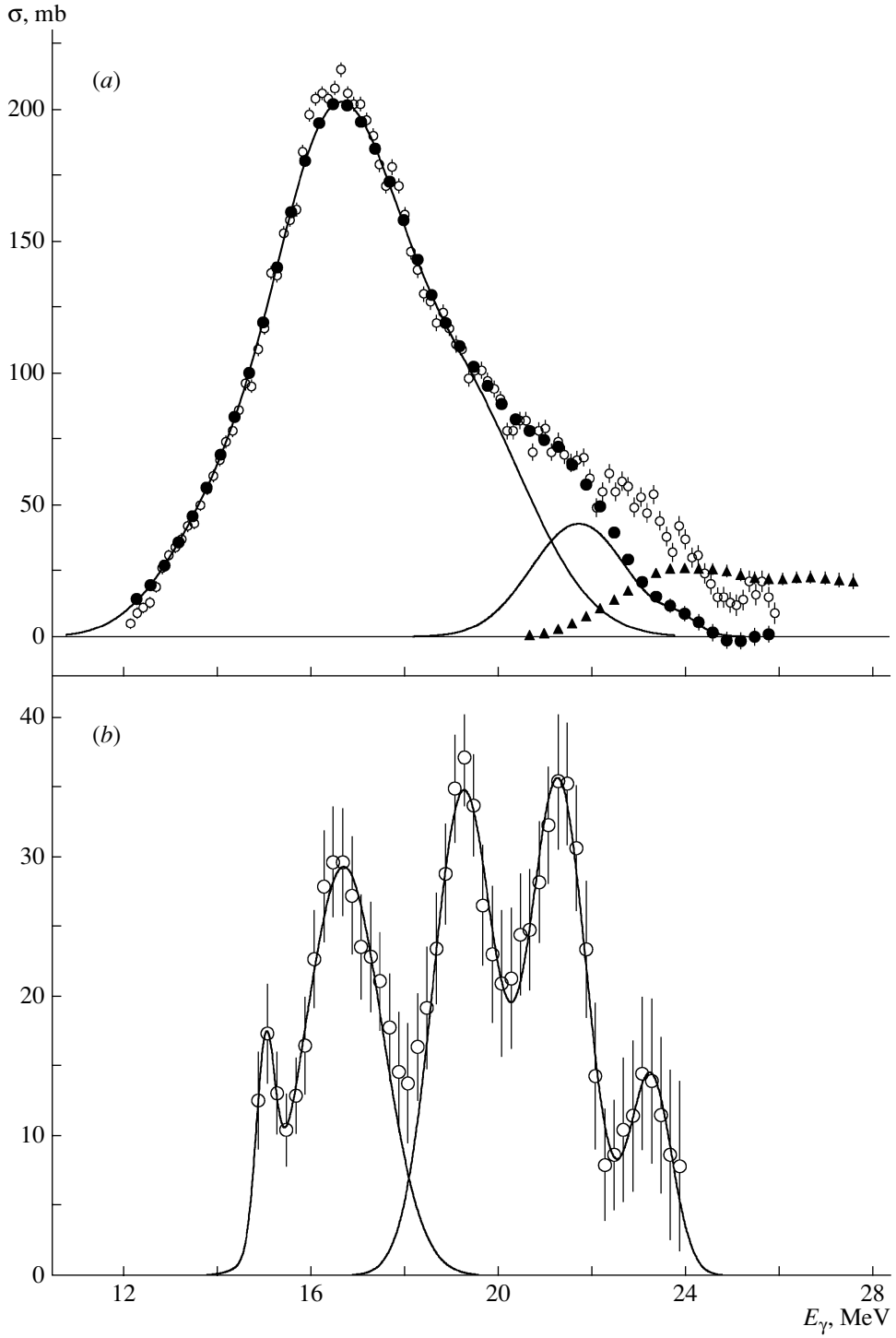

Fig. 8. Approximation of the energy dependences of the cross sections for partial reactions on the ^{90}Zr nucleus by Gaussian functions (the cross-section components corresponding to the isospin values of $T_<$ and $T_>$ are represented by curves): (*a*) (γ, n) cross section {(open circles) data from [17] and (closed circles) cross section corrected in our study; shown additionally (closed triangles) is the $(\gamma, 2n)$ cross section from [17]} and (*b*) (γ, p) cross section.

become even more distinct if, despite all that was said above about five resonances, one approximates the cross sections in question by two curves taken to correspond to two isospin components (Fig. 5)—for the low-energy component, agreement with the experimental cross section is quite satisfactory, but, for the high-energy component, the discrepancy is quite sizable.

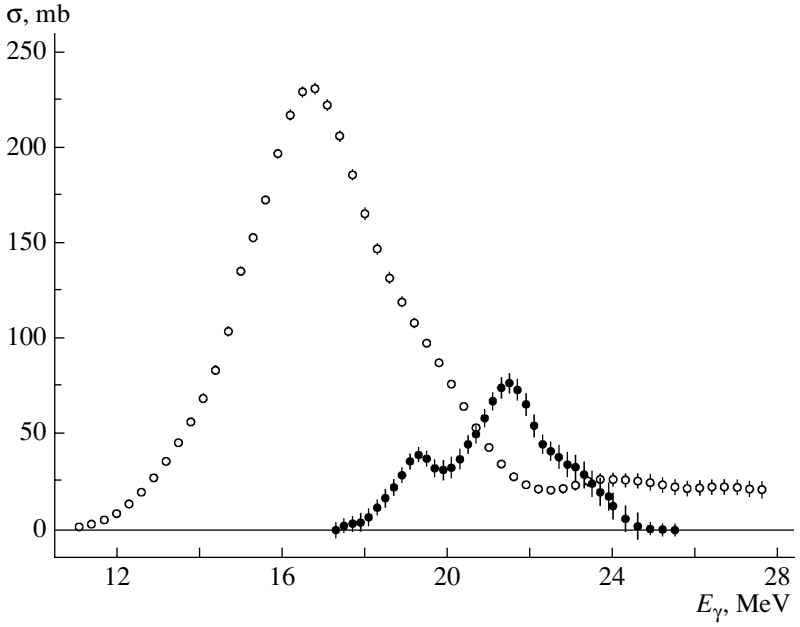

Fig. 9. Isospin-splitting components of the ^{90}Zr(γ, abs.) total-photoabsorption cross section: (open circles) $T_<$ component and (closed circles) $T_>$ component.

The presence of drawbacks such as the "loss" of one of the five resonances clearly manifesting themselves in the cross section, a rather large value of χ^2, and an obviously distorted description of the experimental cross section in the region of high energies invalidates absolutely the further use of approximations by Lorenzian functions (14). In the following, we only employ the results of approximating experimental cross sections by Gaussian functions (13).

4.3. Interpretation of the Isospin Components of the Cross Sections for the Reactions $^{90}Zr(\gamma,\ p)^{89}Y$, $^{90}Zr(\gamma,\ n)^{89}Zr$, and $^{90}Zr(\gamma, 2n)^{88}Zr$

Cross section for the reaction ^{90}Zr(γ, p)^{89}Y. Since the break point in the energy dependence of the ratio $r = \sigma(\gamma,\ p)/\sigma(\gamma,\ n)$ occurs at an energy of about 17.7 MeV (Fig. 6), it follows from the aforesaid that the above isospin interpretation of the cross section for the reaction ^{90}Zr($\gamma,\ p$)^{89}Y is quite straightforward. The first two maxima (those at energies of 15.1 and 16.7 MeV) are expected to be associated with the decay of predominantly $T_<$ states, but, for the next three states (those at energies of 19.3, 21.3, and 23.3 MeV), an increasing role of $T_>$ states must be observed.

Cross section for the reaction ^{90}Zr(γ, n)^{89}Zr. The isospin components of the cross section for the reaction ^{90}Zr($\gamma,\ n$)^{89}Zr can be interpreted in a similar way, but attention should be given to an additional circumstance associated with the relative position (see Fig. 7) of different-isospin states in the ^{90}Zr nucleus and the nuclei neighboring it [28].

The point is that, according to the scheme in Fig. 7, the decay of states of the ^{90}Zr nucleus that have the isospin of $T_> = 6$ through the neutron channel is possible only starting from the energy of 20.2 MeV [28], the threshold for the excitation of states in the neighboring nucleus ^{89}Zr that have the isospin of $T_> = 5\frac{1}{2}$. The decay of states of the ^{90}Zr nucleus that have the isospin of $T_> = 6$ to levels of the ^{89}Zr nucleus that have the isospin of $T_< = 4\frac{1}{2}$ is forbidden by isospin selection rules. Thus, the decay of the ^{90}Zr nucleus through the neutron channel up to energies of about 20.2 MeV may be associated only with isospin-$T_<$ states. It follows that, in contrast to the isospin interpretation of the photoproton cross section, this interpretation for the photoneutron cross section is as follows: the first three maxima, those at energies of 13.8, 16.5, and 19.4 MeV, are due to the decay of predominantly isospin-$T_<$ states, while the next two maxima, those at energies of 21.7 and 23.9 MeV, stem from the decay of isospin-$T_>$ states.

Cross section for the reaction ^{90}Zr(γ, $2n$)^{88}Zr. From the scheme in Fig. 7, it follows that, in the excitation-energy region being considered, the ^{90}Zr decay chain that is necessary for the occurrence of the respective ($\gamma,\ 2n$) reaction and which ends in the formation of states of the ^{88}Zr nucleus that have the isospin of $T_< = 4$ may proceed, according to isospin selection rules, only through levels of the ^{89}Zr nucleus

Table 5. Parameters of the isospin components of the giant dipole resonance in the ^{90}Zr nucleus

Parameters	$T_<$ component	$T_>$ component
Amplitude σ [mb]	231.0	80.7
Width [MeV]	4.1	3.2
Centroid position [MeV]	17.9 (1)	21.2 (1)
Integration range [MeV]	11.1–27.6	17.3–25.8
Integrated cross section $\sigma^{\rm int}$ [MeV mb]	1216.5 (58)	242.3 (70)
First moment $\sigma^{\rm int}_{-1}$ [mb]	69.9 (37)	11.48 (32)

Table 6. Parameters of the ^{90}Zr GDR isospin splitting

Reaction	T	$E_{\rm c.}$, MeV	ΔE, MeV	$\sigma^{\rm int}$, MeV mb	$\sigma^{\rm int}/1.1\times 60NZ/A$	$\sigma^{\rm int}/60NZ/A$	σ_{-1}, mb	R, arb. units
(γ, abs.)	$T_>$	21.2 (1)	**3.3 (2)**	242.3(70)	**0.17**	**0.18**	11.6(3)	**0.14**
	$T_<$	17.9 (1)		1216.5(58)	**0.83**	**0.92**	69.9(4)	
(γ, p)	$T_>$	20.6 (1)		126.8(53)	0.087	0.095	6.2(3)	
	$T_<$	16.6 (1)		65.7(33)	0.045	0.049	4.0(2)	
(γ, n)	$T_>$	21.8 (1)		113.9(32)	0.078	0.085	5.2(1)	
	$T_<$	17.1 (1)		1013.4(22)	0.69	0.760	60.0(3)	
(γ, $2n$)	$T_>$	–	–	–	–	–	–	
	$T_<$	24.9 (1)		130.3(27)	0.09	0.098	5.3(1)	

Table 7. Results of various investigations of ^{90}Zr GDR isospin splitting

	Theoretical estimates [2, 4]	[15, 16]	Our study
ΔE [MeV]	4.0	3.7	3.3
R [arb. units]	0.17	0.10	0.14
$E^{\rm c.}_>$ [MeV]		20.7	21.2
$E^{\rm c.}_<$ [MeV]		16.7	17.9

that have the isospin of $T_< = 4\frac{1}{2}$ and, hence, may start only from levels of the ^{90}Zr nucleus that have the isospin of $T_< = 5$. Thus, the cross section for the reaction ^{90}Zr(γ, $2n$)^{88}Zr is due entirely to the decay of isospin-$T_<$ states of the ^{90}Zr nucleus.

Cross section for the reaction ^{90}Zr(γ, np)^{88}Y. For the sake of completeness of the pattern of isospin splitting in the ^{90}Zr nucleus, it is also necessary to analyze the possible decay chains going through nuclear states characterized by different isospin values and involved in the relevant (γ, np) reaction. This reaction can make different contributions in different energy regions, since it has two possible channels, ^{90}Zr(γ, n)^{89}Zr(γ, p)^{88}Y and ^{90}Zr(γ, p)^{89}Y(γ, n)^{88}Y. According to data from [29], the cross section determined for the reaction ^{90}Zr(γ, np)^{88}Y in the energy region below 31 MeV is about 2 mb—that is, it is an order of magnitude smaller than the cross section for the reaction ^{90}Zr(γ, $2n$)^{88}Zr, the latter being about 20 mb (the integrated cross sections are 14 and 141 MeV mb, respectively). This gives sufficient grounds to believe that the contribution of the respective (γ, np) reaction to the isospin splitting of the giant dipole resonance in the ^{90}Zr nucleus is insignificant.

The results obtained by the method outlined above for the isospin components of all cross sections under discussion for the photodissociation of the ^{90}Zr nucleus are given in Fig. 8.

Figure 9 displays both isospin components of the total-photoabsorption cross section obtained with allowance for the rescaling [22] of the cross sections from [17] for the reactions ^{90}Zr(γ, n)^{89}Zr and ^{90}Zr(γ, $2n$)^{88}Zr. The parameters of both isospin components of the giant dipole resonance in the ^{90}Zr

nucleus are given in Table 5, while the results determined from them for the parameters of the isospin splitting of the giant dipole resonance in the ^{90}Zr nucleus are quoted in Table 6 (printed in boldface) along with the parameters of the isospin components of cross sections for partial reactions.

5. COMPARISON OF THE RESULTS OF OUR STUDY AND PREVIOUS EXPERIMENTAL AND THEORETICAL STUDIES

The results obtained in the present study and in [15, 16] for the basic parameters of the GDR isospin splitting in the ^{90}Zr nucleus are quoted in Table 7 along with respective theoretical estimates from [2, 4].

Our results are indicative of the following:

(i) Both isospin components identified in our study are shifted toward higher energies in relation to data from [15, 16].

(ii) The $T_<$ component is shifted stronger (1.2 MeV) than the $T_>$ component (0.5 MeV), this reducing the isospin-splitting value (3.3 instead of 3.7 MeV).

(iii) The isospin-splitting value obtained in [15, 16] (3.7 MeV) is somewhat closer to the theoretical value (4.0 MeV) than the result obtained here (3.3 MeV).

(iv) The ratio of the intensities of isospin components, R, that was obtained in the present study (0.14 arb. units) proves to be much closer to the theoretical estimate (0.17 arb. units) than the data from [15, 16].

From the foregoing, it follows that all of the aforementioned discrepancies between experimental data and theoretical estimates can be attributed to the same factors—specifically, the mutual correction of the cross sections for $(\gamma,\ n)$ and $(\gamma,\ 2n)$ reactions and the absence of a correct calculation of the contribution from the reaction $^{90}\mathrm{Zr}(\gamma,\ 2n)^{88}\mathrm{Zr}$ in [2, 4, 15, 16].

(i) It has been shown that, in the experiment reported in [17] and devoted to determining cross sections for $(\gamma,\ n)$ and $(\gamma,\ 2n)$ reactions, the contribution of the former was sizably (unjustifiably) overestimated, while the contribution of the latter was strongly underestimated; in evaluating the parameters of isospin splitting in [15, 16], the cross section for the former reaction was taken into account, while the contribution of the latter was disregarded. The correction (Fig. 4) of the cross sections for the two reactions [22] [a considerable enhancement of the $(\gamma,\ 2n)$ cross section via the reduction of the $(\gamma,\ n)$ cross section] leads to effects precisely of the type indicated above (see Table 7).

(ii) In theoretical estimates, no account was taken of the factor associated with the cross section for the reaction $^{90}\mathrm{Zr}(\gamma,\ 2n)^{88}\mathrm{Zr}$—the concept of GDR isospin splitting was based on the assumption that the Coulomb interaction is much weaker than the nuclear interaction, this being characteristic of heavy nuclei. In the photodisintegration of heavy nuclei, the contribution of $(\gamma,\ 2n)$ reactions is much less pronounced than the contribution of $(\gamma,\ n)$ reactions, but this is not so for medium-mass nuclei, which include the ^{90}Zr nucleus; as a result, a simple geometric approach to interpreting the proton and neutron channels of giant-resonance-decay as the decay of states of the intermediate nucleus that have different isospin values is not fully justified.

The particular role of $(\gamma,\ 2n)$ reactions in the region of not very heavy nuclei is worthy of special note. It was shown above that, by virtue of the relationship between the thresholds for the excitation of states having appropriate isospin values in nuclei featuring N, $N-1$, and $N-2$ neutrons, the $(\gamma,\ 2n)$ reaction for ^{90}Zr can proceed only through $T_<$ states according to the following scheme: $T = 5 \to T = 9/2 \to T = 4$. Since the threshold for the $(\gamma,\ 2n)$ reaction is much higher than the threshold for the $(\gamma,\ np)$ reaction and since their cross sections are commensurate in absolute value, this situation changes the concept of the isospin splitting of giant dipole resonances for nuclei of the zirconium region on the whole: a rather large number of isospin-$T_>$ states prove to be immersed in isospin-$T_<$ states, which are situated both at lower and at higher energies. Naturally, the common spreading of dipole states (giant-dipole-resonance width) then becomes even larger than the value predicted by the above isospin-splitting concept, but the splitting value as estimated by the difference of the positions of the energy centroids of different-isospin states proves to be smaller. The ratio of the intensities of the isospin components, R, also differs significantly from theoretical estimates, since, in estimating it within the concept of the isospin splitting of giant dipole resonances, no account was taken of the contributions from $(\gamma,\ 2n)$ reactions.

ACKNOWLEDGMENTS

We are grateful to Professors B.S. Ishkhanov and M.H. Urin and to I.N. Boboshin and I.V. Safonov for stimulating discussions.

This work was performed at the Centre for Photonuclear Experiments Data of the Division of Electromagnetic Processes and Atomic Nuclei Interactions at the Skobeltsyn Institute of Nuclear Physics of Lomonosov Moscow State University and was supported by RF state contract no. 02.51312.0046.

REFERENCES

1. V. V. Varlamov, B. S. Ishkhanov, and M. E. Stepanov, Izv. RAN, Ser. Fiz. **62**, 1035 (1998).
2. S. Fallieros, B. Goulard, and R. H. Venter, Phys. Lett. **19**, 398 (1965).
3. R. Leonardi, Phys. Rev. Lett. **28**, 836 (1972).
4. R. O. Akyuz and S. Fallieros, Phys. Rev. Lett. **27**, 1016 (1971).
5. H. Morinaga, Phys. Rev. **97**, 444 (1955).
6. V. V. Varlamov, N. G. Efimkin, B. S. Ishkhanov et al., Yad. Fiz. **58**, 387 (1995) [Phys. At. Nucl. **58**, 337 (1995)].
7. V. V. Varlamov, N. G. Efimkin, B. S. Ishkhanov, et al., Izv. Akad. Nauk, Ser. Fiz. **59**, 223 (1995).
8. K. G. McNeill, M. N. Thompson, A. D. Bates, et al., Phys. Rev. C **47**, 1108 (1993).
9. V. V. Varlamov, B. S. Ishkhanov, I. M. Kapitonov, et al., Nucl. Phys. A **222**, 548 (1974).
10. V. V. Varlamov and M. E. Stepanov, Preprint No. 99-40/598 (Inst. Yad. Fiz., Mosk. Gos. Univ., Moscow, 1999).
11. V. V. Varlamov, B. S. Ishkhanov, I. M. Kapitonov, et al., Vestn. MGU, Ser. Fiz. Astron., No. 3, 297 (1976).
12. V. V. Varlamov, B. S. Ishkhanov, I. M. Kapitonov, et al., Izv. AN SSSR, Ser. Fiz. **39**, 1744 (1975).
13. B. S. Ishkhanov, I. M. Kapitonov, V. G. Shevchenko, et al., Nucl. Phys. A **283**, 307 (1977).
14. V. V. Varlamov and M. E. Stepanov, Yad. Fiz. **65**, 52 (2002) [Phys. At. Nucl. **65**, 49 (2002)].
15. K. Shoda, H. Miyase, M. Sugawara, et al., Nucl. Phys. A **239**, 397 (1975).
16. K. Shoda, Phys. Rep. **53**, 343 (1979).
17. A. Lepretre, H. Beil, R. Bergere, et al., Nucl. Phys. A **175**, 609 (1971).
18. E. Wolynec, A. R. V. Martinez, P. Gouffon, et al., Phys. Rev. C **29**, 1137 (1984).
19. E. Wolynec and M. N. Martins, Rev. Bras. Fis. **17**, 56 (1987).
20. V. V. Varlamov, N. G. Efimkin, N. A. Lenskaja, and A. P. Chernjaev, Preprint No. 89-66/143 (Inst. Nucl. Phys., Mosk. Gos. Univ, Moscow, 1989).
21. V. V. Varlamov and B. S. Ishkhanov, INDC(CCP)-433, IAEA NDS (Vienna, Austria, 2002).
22. V. V. Varlamov, N. N. Peskov, D. S. Rudenko, M. E. Stepanov, VANiT, Ser. Yad. Konstanty, No. 1, 2, 48 (2003).
23. Nuclear-Reaction Database (EXFOR), CDFE, Inst. Yad. Fiz., Mosk. Gos. Univ., http://cdfe.sinp.msu.ru/exfor/index.php.
24. S. S. Dietrich and B. L. Berman, At. Data Nucl. Data Tables **38,** 199 (1988).
25. W. W. Gargaro and D. S. Onley, Phys. Rev. C **4**, 1032 (1971).
26. C. W. Soto Vargas, D. S. Onley, and L. E. Wright, Nucl. Phys. A **288**, 45 (1977).
27. W. R. Dodge, E. Hayward, and E. Wolynec, Phys. Rev. C **28**, 150 (1983).
28. Complete Nuclear Spectroscopy Database "Relational ENSDF" CDFE, Inst. Yad. Fiz., Mosk. Gos. Univ., http://cdfe.sinp.msu.ru/services/ensdfr.html.
29. D. Brajnik, D. Jamnik, G. Kernel, et al., Phys. Rev. C **13**, 1852 (1976).

Translated by A. Isaakyan